Journal of Photonics for Energy

PhotonicsforEnergy.SPIEDigitalLibrary.org

Interface structure between titania and perovskite materials observed by quartz crystal microbalance system

Soya Nakayashiki
Hirotani Daisuke
Yuhei Ogomi
Shuzi Hayase

SPIE.

Interface structure between titania and perovskite materials observed by quartz crystal microbalance system

Soya Nakayashiki, Hirotani Daisuke, Yuhei Ogomi, and Shuzi Hayase*
Kyushu Institute of Technology, 204 Hibikino Wakamatsu-ku, Kitakyushu 808-0196, Japan

Abstract. Adsorption of PbI_2 onto a titania layer was monitored by a quartz crystal microbalance system in solution. The amount of PbI_2 adsorbed on the titania layer increased with an increase in the PbI_2 concentration in dimethylformamide (DMF). However, PbI_2 remained after being rinsed with DMF, suggesting that PbI_2 is rigidly bonded to the surface of the titania. The x-ray photoelectron spectroscopy measurement of PbI_2 adsorbed on the titania substrate showed that the Pb compound has a composition of $PbI_{0.33}$, not PbI_2, suggesting that part of the Pb-I reacts with the HO-Ti moieties of titania to form Pb-O-Ti linkages. Trap density as measured by the thermally stimulated current method decreased after PbI_2 passivation. Perovskite solar cells consisting of porous titania passivated with PbI_2 had a higher efficiency than those without the passivation. It was concluded that PbI_2 passivation of porous titania surfaces is one of the crucial approaches for enhancing the efficiency of perovskite solar cells with a scaffold layer of porous titania. [DOI: 10.1117/1.JPE.5.057410]

Keywords: perovskite solar cells; quartz crystal microbalance; interface; passivation; PbI_2.

Paper 14102SS received Nov. 18, 2014; accepted for publication Feb. 27, 2015; published online Mar. 25, 2015.

1 Introduction

The certified efficiency of perovskite solar cells with a size of 0.1 cm^2 is now 17.8% (Ref. 1) and comes close to the 20.4% efficiency of polycrystalline Si solar cells. Therefore, perovskite solar cells are expected to be one of the important types of solar cells in the next generation printable solar cells. Perovskite solar cells contain $CH_3NH_3PbI_3$ (Perov Pb) as the light harvesting layer.[2–9] The Perov Pb layer is prepared by spin-coating the mixture of $PbCl_2$ (or PbI_2) and CH_3NH_3I (MAI) onto a TiO_2 nanoporous layer (scaffold layer); this process is known as a one-step synthesis.[3] The Perov Pb can also be prepared with a two-step synthesis, where the PbI_2 layer is fabricated on a porous titania layer (scaffold layer) and the sample is dipped in the MAI solution in dimethylformamide (DMF). The MAI is diffused in the PbI_2 layer to make the perovskite structures.[4] It has been reported that the two-step process has the advantage of a higher efficiency over the one-step process.[4] In this report, we focus on the two-step process. When the perovskite layer is exposed to light, the perovskite is excited and electrons are injected into the titania layer or are carried by the perovskite itself.[5,6,9] The surface of the porous titania affects the electron collection as well as the crystal growth of the perovskite crystals.[10–12] For example, we have reported that the electron trap density of the perovskite/titania layer is decreased by passivating the surface of the titania.[10,12] In addition, the crystal size of the perovskite becomes larger when the titania surface is passivated with amino acid hydroiodic acid (HI) salt.[11] The interface between titania and the perovskite crystal is crucial for understanding the photoconversion; however, the interface has not been discussed in detail. Previously, dye adsorption for dye-sensitized solar cells has been discussed using a quartz crystal microbalance (QCM) measurement.[13,14] We now discuss the interface structure of the titania/perovskite layer by monitoring the PbI_2 adsorption on the titania layer employing the QCM measurement.

*Address all correspondence to: Shuzi Hayase, E-mail: hayase@life.kyutech.ac.jp

2 Experimental

PbI_2 and CH_3NH_3I were prepared in the same way as has been reported in previous works.[10–12] Figure 1 shows the QCM system (Meywafosus Co. LTD) employed in this experiment. The titania (anatase) compact layer (500 nm) was prepared on a Au QCM sensor by atomic layer deposition (ALD) (Sunable ALD R200 Basic, Picosun) using $TiCl_4$ and water as the precursor. The chamber temperature was kept at 300°C (1000 cycles, 50 nm thickness), followed by annealing the sample at 450°C for 30 min. The titania compact layers had an anatase structure. The titania/Au sensor was placed at position B in Fig. 1. The PbI_2 solution in the DMF (0.2 to 5 mM) was put into container A, and the solution was passed over the titania/QCM sensor B. The flow rate was 0.5 μL/s and the temperature was kept at 25°C. The amount of PbI_2 adsorbed on the titania compact layer was monitored with a frequency shift according to the following Sauerbrey equation:[15]

$$\Delta F = \frac{2F_0^2}{\sqrt{\rho\mu}}\frac{\Delta m}{A}, \tag{1}$$

where ΔF is the frequency change, F_0 is the sensor frequency, Δm is the change of weight, A is the sensor area, μ is the shearing stress (2.947×10^{10} kg ms), and ρ is the density (2648 kg/m^3).

The perovskite solar cell was prepared in the same way as in our previous reports.[10–12] F-doped SnO_2 layered glass (FTO glass, Nippon Sheet Glass Co. Ltd.) was patterned using Zn and a 6 M HCl aqueous solution. On this patterned FTO glass, titanium diisopropoxide bis(acetylacetonate) solution in ethanol was sprayed at 300°C to prepare the compact titania layers. A porous titania layer was fabricated by spin-coating titania paste (PST-18NR, JGC Catalysts and Chemicals Ltd.) in ethanol (titania paste:ethanol = 1:2.5 weight ratio), followed by heating the substrate at 550°C for 30 min. The one-step preparation process for perovskite solar cells is as follows: MAI and PbI_2 were mixed in a 1:1 molar ratio to prepare a 40% solution of perovskite in N,N-dimethylformamide (DMF) and the mixture was spin-coated on the substrate. The substrate was heated at 100°C for 45 min, followed by spin-coating a mixture of 55 mM of tert-butylpyridine, 9 mM of lithium bis(trifluoromethylsyfonyl)imide salt, and 68 mM of 2,2',7,7'- tetrakis[N,N-di (4-methoxy phenyl) amino]—9,9'- spirobifluorene (spiro). Finally, Ag and Au electrodes were fabricated with a vacuum deposition method (ALS Tech E-299).

The two-step preparation process for perovskite solar cells is as follows: 1 M solution of PbI_2 in N,N'-dimethylformamide (DMF) was spin-coated, followed by baking at 70°C for 30 min. After that, the sample was dipped in a 10 mg/ml solution of MAI in 2-propanol for 30 s. After rinsing, the sample was heated at 70°C for 30 min. On the sample, spiro and electrode were prepared in the same way as in the one-step preparation. The photovoltaic performance of the cells was evaluated using an AM 1.5G 100 mW/cm^2 irradiance solar simulator (CEP-2000, Bunkoukeiki Inc.) and a 0.4×0.4 cm^2 mask on a cell of size 0.5×0.5 cm^2.

The thermally stimulated current (TSC) was measured using a TS-FETT apparatus (Rigaku) in the same way as described in our previous reports.[16] At a low temperature (−180°C), traps were filled with electrons by exposing the substrate to ultraviolet light. As the temperature of

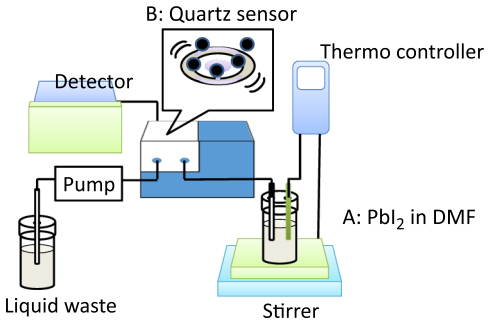

Fig. 1 Quartz crystal microbalance measurement apparatus for measuring PbI_2 adsorption on titania surface.

the sample increased, these electrons were released from the trap sites. These electrons are detected as a TSC. The TSC at a higher temperature is the result of electrons released from deeper traps and the TSC at a lower temperature is associated with electrons released from shallow traps. The trap depths and trap densities are calculated using the temperature and the current density at that temperature by Eqs. (2) and (3), respectively.[16,17]

$$E_t = kT_m \times \ln(T_m^4/\beta), \tag{2}$$

where E_t is the trap depth, k is the Boltzmann constant, T_m is the temperature (K), β is the programing rate (K/s), and ln is the natural logarithm

$$N = (dI/dt) \times (1/enP), \tag{3}$$

where N is the trap density, dI/dt is the current/unit time, e is the elementary charge, n is the volume (thickness × gap), and P is the porosity.

3 Results and Discussion

Figure 2 shows the relationship between the adsorption time and the PbI_2 adsorption density on a compact titania layer. The PbI_2 solution was introduced to the sensor surface at point A in Fig. 2. The weight of the compact layer increased with time, demonstrating that PbI_2 was adsorbed on the compact titania layer. At point B in Fig. 2, the surface was rinsed by introducing DMF onto the sensor surface. The adsorption curve showed a sharp drop and remained at a constant value after that. The curve was explained as follows. The amount of PbI_2 adsorbed on the compact titania layer increased with time and the uptake speed gradually decreased. Weakly adsorbed PbI_2 was washed away upon rinsing with DMF and strongly adsorbed PbI_2 remained on the titania surface.

The saturated (maximum) PbI_2 adsorption density increased with an increase in the PbI_2 concentration and reached a constant value as shown in Fig. 3, suggesting that PbI_2 was adsorbed on all the adsorption sites. A, B, and C are explained later (Table 1). Supposing that the diameter of PbI_2 is 0.558 to 0.954 nm, the surface area occupied by one PbI_2 molecule is calculated to be 2.45 to 7.15×10^{-15} cm^2. If all surfaces were covered with PbI_2, the adsorption density of PbI_2 could be calculated to be 107 to 313 ng/cm^2. The experimentally determined saturated adsorption density was ~150 to 200 ng/cm^2 as shown in Fig. 3. The experimentally estimated adsorption density was roughly coincident with the calculated value.

The x-ray photoelectron spectroscopy (XPS) of PbI_2 adsorbed on the titania layer is shown in Fig. 4. In Fig. 4(b), the 616 eV peak is assigned to I_{3d}, and both the 135 and 137 eV peaks are assigned to Pb_{4f}, as estimated from the data base shown in Fig. 4(a). The ratio of Pb:I of PbI_2 adsorbed on the titania layer was estimated from the comparison of the peak intensity of a PbI_2 thin film prepared on a glass substrate and was determined to be Pb : I = 1 : 0.03. This suggested

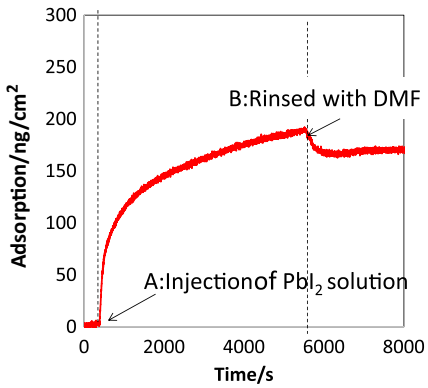

Fig. 2 Relationship between PbI_2 adsorption density on titania and the adsorption time.

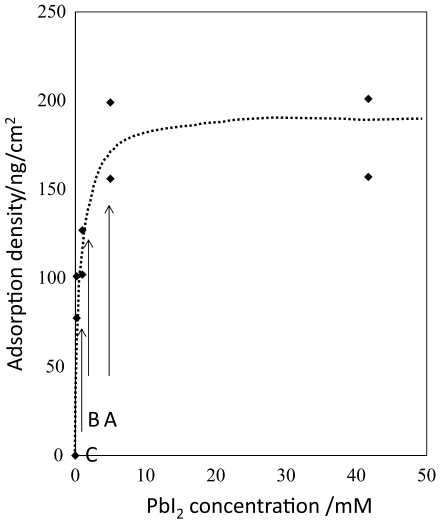

Fig. 3 Relationship between saturated PbI_2 adsorption density and PbI_2 concentration in dimethyl formamide (DMF).

that PbI_2 is bonded on the titania surface by a Pb-O-Ti linkage as shown in Fig. 5. It is probable that Ti-OH moieties on a titania layer react with Pb-I to form Ti-O-Pb and HI, namely; the negatively charged O of Ti-O attacks the positively charged Pb nucleophilically to form Ti-O-Pb.

The Pb_{4f} signals of XPS for a Perov Pb bulk layer and a PbI_2 bulk layer were observed at 135.6 and 135.7 eV, respectively, as shown in Fig. 6. After the bulk layer of the Perov Pb layer and the bulk layer of PbI_2 on the titania layer were washed away, the titania surface was analyzed by XPS. The peak assigned to Pb_{4f} was observed for the rinsed PbI_2/titania surface at 136.4 eV, which was slightly shifted to a higher bonding energy than that of bulk PbI_2 (135.7 eV). This is consistent with previous reports that the metals of an oxide metal have higher XPS bonding energies than that of the corresponding halides. The rinsed Perov Pb/titania surface also has the same XPS peak (136.4 eV) as the rinsed PbI_2/titania layer. This suggests that Ti-O-Pb linkages are also formed at the titania/Perov Pb interfaces as well as at the titania/PbI_2 interfaces. Perov Pb crystals may grow from the Pb-O-Ti surfaces.

In order to examine the surface passivation effects on solar cell performance, the surface of the porous titania was treated with dilute PbI_2 solutions with various concentrations, such as 0.2, 1, and 5 mM. The different concentrations correspond to points A, B, and C in Fig. 3, where 150 to 200, 100 to 125, and ~75 ng/cm^2 of PbI_2 were absorbed on the porous titania surface. After the surface treatment of the titania layer with a PbI_2 dilute solution, the mixed solution of PbI_2 and MAI was spin-coated on the porous titania layer to form a perovskite layer (Perov Pb). The photovoltaic performances for these solar cells are summarized in Table 1, in which the performance for a Perov Pb solar cell without any surface pretreatment is also included. It is observed that the photovoltaic performances, namely, J_{sc} and V_{oc}, increased with an increase in the concentration of PbI_2 passivation from 0.2 to 5 mM as shown in A, B, and C in Fig. 3.

Table 1 Photovoltaic performances for solar cells consisting of $CH_3NH_3PbI_3$.

	J_{SC} (mA/cm^2)	V_{OC} (V)	Fill factor	PCE (%)
One-step (1)	8.45	0.78	0.44	2.91
PbI_2 0.2 mM + One-step (2)	12.14	0.80	0.56	5.47
PbI_2 1 mM + One-step (3)	12.87	0.81	0.59	6.12
PbI_2 5 mM + One-step (4)	13.84	0.80	0.60	6.64
Two-step (5)	14.84	0.84	0.59	7.33

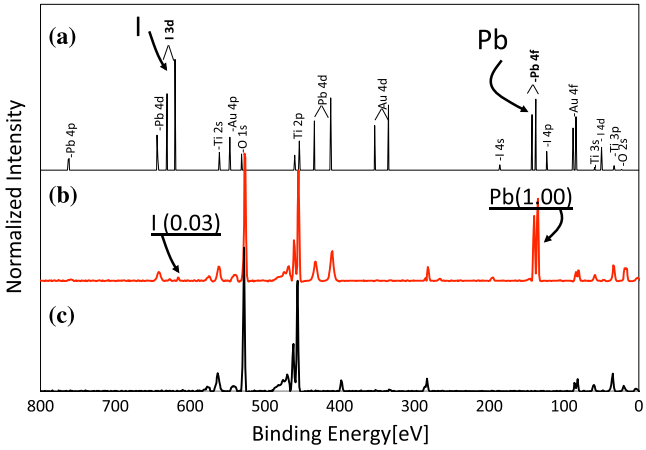

Fig. 4 X-ray photoelectron spectroscopy (XPS) spectra of Pb adsorbed on titania: (a) reference, (b) PbI_2 solution was coated on compact titania layer and the substrate was rinsed with DMF, (c) compact titania only for the reference.

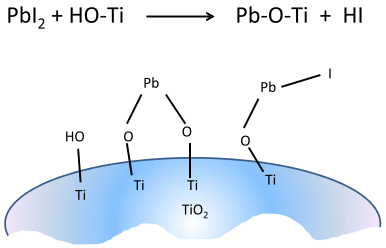

Fig. 5 Expected reaction of PbI_2 and titania.

These results demonstrate that the photovoltaic performances are improved by controlling the titania–perovskite interfaces (passivation effect).

For our experimental conditions, the two-step preparation method showed higher photovoltaic performances (7.33%) than the one-step preparation method (2.91%) as shown in Table 1. In the two-step preparation method, the PbI_2 layer is directly fabricated on the porous titania layer by using a 1 M solution of PbI_2 (a much higher concentration) before MAI is introduced to the PbI_2 layer. Therefore, the interface between the PbI_2 and the porous titania layer was well passivated by the Ti-O-Pb bond formation.

Two possible mechanisms have been proposed for electron collection. One explanation is that electrons are collected through the nanoporous titania, which is a mechanism similar to

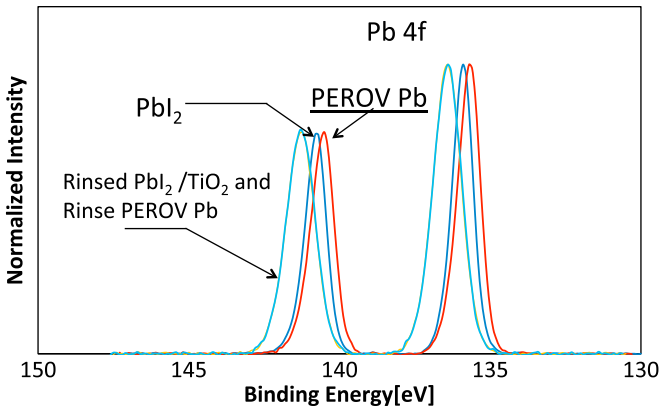

Fig. 6 XPS Pb_{4f} signal of Pb adsorbed on titania surface.

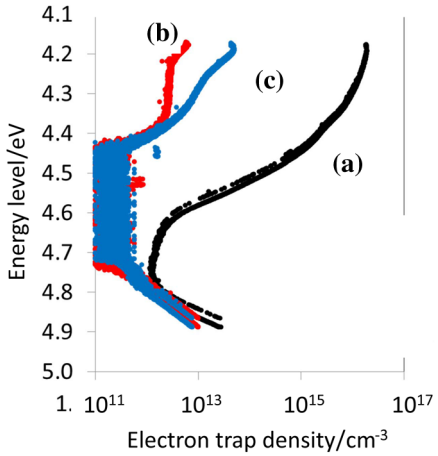

Fig. 7 Trap distributions of TiO_2 passivated with and without PbI_2: (a) titania only, (b) porous titania passivated with PbI_2, (c) PbI_2/porous titania after being rinsed with DMF.

that of dye-sensitized solar cells.[4] The other explanation is that electrons are directly collected by the Perov Pb layers.[5] For a Perov Pb solar cell consisting of porous titania, both processes may occur simultaneously. In Perov solar cells consisting of porous titania layer, electrons would be collected by both of porous titania layer and Perob Pb layer.[16] Since these traps become charge recombination centers, the trap density must be low.[18–23] Figure 7 shows the electron trap distribution for the titania porous layer, the titania/PbI_2 layer, and the titania/PbI_2 rinsed with DMF solution. The trap density of porous titania at −4.2 eV was $10^{16}/cm^3$ and the trap density decreased to 10^{12} and 10^{11} after the porous titania surface was passivated with PbI_2. Even after the surface was rinsed with the DMF solution, a low trap density was maintained, demonstrating that the titania surface was passivated with Ti-O-Pb linkages by PbI_2.

4 Conclusion

The interface structure between titania and a Perov Pb layer was examined by QCM, XPS, and thermally stimulated currents. It was concluded that the interface was made by Ti-O-Pb, which passivates the surface trap of nanoporous titania. The photovoltaic performances were improved after the passivation.

Acknowledgments

This work was supported by Funding Program for the World–Leading Innovative R&D on Science and Technology (FIRST program headed by Professor Hiroshi Segawa).

References

1. M. A. Green et al., "Solar cell efficiency tables (Version 45)," *Prog. Photovolt: Res. Appl.* **22**, 701–710 (2014).
2. J. H. Noh et al., "Chemical management for colorful, efficient, and stable inorganic–organic hybrid nanostructured solar cells," *Nano Lett.* **13**, 1764–1769 (2013).
3. H.-S. Kim et al., "Lead iodide perovskite sensitized all-solid-state submicron thin film mesoscopic solar cell with efficiency exceeding 9%," *Sci. Rep.* **2**, 591 (2012).
4. J. Burschka et al., "Sequential deposition as a route to high-performance perovskite-sensitized solar cells," *Nature* **499**, 316–319 (2013).
5. M. M. Lee et al., "Efficient hybrid solar cells based on meso-superstructured organometal halide perovskites," *Science* **338**, 643–647 (2012).
6. J. M. Ball et al., "Low-temperature processed mesosuperstructured to thin-film perovskite solar cells," *Energy Environ. Sci.* **6**, 1739–1743 (2013).

7. D. Liu and T. L. Kelly, "Perovskite solar cells with a planar heterojunction structure prepared using room-temperature solution processing techniques," *Nat. Photonics* **8**, 133–138 (2013).
8. H. J. Snaith, "Perovskites: the emergence of a new era for low-cost, high-efficiency solar cells," *J. Phys. Chem. Lett.* **4**, 3623–3630 (2013).
9. M. Liu, M. B. Johnston, and H. J. Snaith, "Efficient planar heterojunction perovskite solar cells by vapour deposition," *Nature* **501**, 395–398 (2013).
10. Y. Ogomi et al., "Control of charge dynamics through a charge-separation interface for all-solid perovskite-sensitized solar cells," *ChemPhysChem.* **15**, 1062–1069 (2014).
11. Y. Ogomi et al., "All-solid perovskite solar cells with HOCO-R-NH3+I- anchor-group inserted between porous titania and perovskite," *J. Phys. Chem.* **118**, 16651–16659 (2014).
12. Q. Shen et al., "Charge transfer and recombination at the metal oxide/CH3NH3PbClI2/spiro-OMeTAD interfaces: uncovering the detailed mechanism behind high efficiency solar cells," *ChemPhysChem.* **15**, 1062–1069 (2014).
13. H. A. Harms et al., "*In situ* investigation of dye adsorption on TiO_2 films using a quartz crystal microbalance with a dissipation technique," *Phys. Chem. Chem. Phys.* **14**, 9037–9040 (2012).
14. H. A. Harms et al., "*In-situ* investigation of adsorption of dye and coadsorbates on TiO_2 films using QCM-D fluorescence and AFM techniques," *Proc. SPIE* **8811**, 88110C (2013).
15. K. K. Kanazawa and J. G. Gordon, "Frequency of a quartz microbalance in contact with liquid," *Anal. Chem.* **57**, 1770–1777 (1985).
16. Y. Noma et al., "Surface state passivation effect for nanoporous TiO_2 electrode evaluated by thermally stimulated current and application to all-solid state dye-sensitized solar cells," *Jpn. J. Appl. Phys.* **47**, 505 (2008).
17. A. Opanowicz and P. Petrucha, "Heating-rate method for determination of kinetic parameters from thermally stimulated conductivity and luminescence," *J. Appl. Phys.* **93**, 957–967 (2003).
18. A. Kay and M. Grätzel, "Dye-sensitized core–shell nanocrystals: improved efficiency of mesoporous tin oxide electrodes coated with a thin layer of an insulating oxide," *Chem. Mater.* **14**, 2930–2935 (2002).
19. Y. Diamant et al., "Core–shell nanoporous electrode for dye sensitized solar cells: the effect of shell characteristics on the electronic properties of the electrode," *Coord. Chem. Rev.* **248**, 1271–1276 (2004).
20. E. Palomares et al., "Control of charge recombination dynamics in dye sensitized solar cells by the use of conformally deposited metal oxide blocking layers," *J. Am. Chem. Soc.* **125**, 475–482 (2003).
21. F. Fabregat-Santiago et al., "Electron transport and recombination in solid-state dye solar cell with spiro-OMeTAD as hole conductor," *J. Am. Chem. Soc.* **131**, 558–562 (2009).
22. F. Fabregat-Santiago et al., "The origin of slow electron recombination processes in dye-sensitized solar cells with alumina barrier coatings," *J. Appl. Phys.* **96**, 6903–6907 (2004).
23. Y. Ogomi et al., "Ru dye uptake under pressurized CO_2 improvement of photovoltaic performances for dye-sensitized solar cells," *J. Electrochem. Soc.* **153**, A2294–A2297 (2006).

Shuzi Hayase graduated from Osaka University in 1978 and received his PhD from Osaka University in 1983. He was with the R&D Center at Toshiba from 1978 to 2000, during which he engaged in the development of ULSI lithography. He was with the polysilane research group of the Robert West group at the University of Wisconsin from 1988 to 1990. He has been a professor at the Kyushu Institute of Technology (National Institute) since 2001. His research interest is printable solar cells and their materials.

Biographies of the other authors are not available.